Spectroscopic study of plasma during electrolytic oxidation of magnesium-aluminium alloys

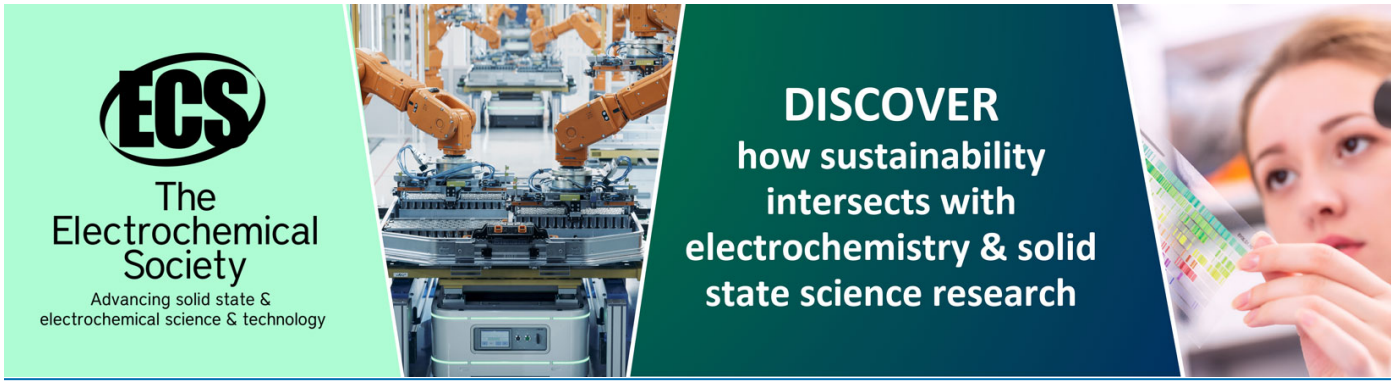

Journal of Physics: Conference Series **565** (2014) 012013 doi:10.1088/1742-6596/565/1/012013

Spectroscopic study of plasma during electrolytic oxidation of magnesium-aluminium alloys

J Jovović
University of Belgrade, Faculty of Physics, Studentski trg 12-16, 11001 Belgrade, Serbia

E-mail: jjovica@ff.bg.ac.rs

Abstract. Plasma during Electrolytic Oxidation (PEO) of magnesium-aluminium alloys is studied in this work by means of Optical Emission Spectroscopy (OES). Spectral line shapes of the H_β, Al II 704.21 nm and Mg II 448.11 nm line are analyzed to measure plasma electron number density N_e. From the H_β line profile, two PEO processes characterized by relatively low electron number densities $N_e \approx 10^{15}$ cm^{-3} and $N_e \approx 2 \times 10^{16}$ cm^{-3} were discovered while the shape and shift of Al II and Mg II lines revealed the third process characterized by large electron density N_e = (1-2) × 10^{17} cm^{-3}. Low N_e processes, related with breakdown in gas bubbles and on oxide surface, are not influenced by anode material or electrolyte composition. The ejection of evaporated anode material through oxide layer is designated here as third PEO process.
Using the Boltzmann plot technique, electron temperature of 4000 K and 33000 K is determined from relative intensities of Mg I and O II lines, respectively. Several difficulties in the analysis of spectral line shapes are met during this study and the ways to overcome some of the obstacles are demonstrated.

1. Introduction

Plasma electrolytic oxidation (PEO) is high-voltage anodizing technique which produces a stable oxide coating on the surface of metals and metallic alloys, see e.g. [1] and references therein. PEO is characterized by local formation of plasma, as indicated by the presence of micro-discharges on the metal/oxide surface accompanied by gas evolution. Short-lived micro-discharge events determine thermal and chemical conditions and play an important role in the phase formation, composition and morphology of metal oxide coating [2,3,4].

The study of PEO is often realized using OES, see e.g. [5] and references therein. This approach is however followed by difficulties due to space and time inhomogeneity of micro-discharges appearing randomly across the anode surface, see e.g. [6]. In that case, the recorded spectra represent time integrated low intensity radiation for which long exposure times during spectroscopic observations of PEO are necessary. Hence, the application of OES for PEO diagnostics is mostly limited to spectra identification and observation of temporal evolution of spectral lines in a visible and near UV region.

The PEO spectra recorded from aluminium [5], tantalum [7] and titanium [8] samples in various electrolytes were recently studied. The analysis of the H_α and the H_β line shapes showed that two plasma processes are always present in PEO micro-discharges. During PEO of aluminium, the third discharge process appears followed by evaporation of anode material and formation of aluminium plasma [5]. With tantalum [7] and titanium [8], local evaporation of anode does not occur and consequently spectral lines of anode material were not detected. In this study the focus was on the

third process – metal plasma ejection through oxide layer. Therefore, two magnesium-aluminium alloys are used as anode material. The selected alloys have dominant concentration of either Mg or Al, the elements with almost same low melting temperature (Mg: T_m = 650 °C, Al: T_m = 660 °C). This is of importance for metal plasma generation after evaporation of anode material. Also, Mg and Al have much lower melting point than Ti (T_m = 1668 °C) and Ta (T_m = 3017 °C), which do not melt during PEO process [7,8]. The electron number density (N_e) is measured from the shape of the H_β line and from the Stark broadening parameters of Mg II and Al II lines while electron temperature (T_e) required for N_e measurement will be determined from relative intensities of Mg I and O II lines using Boltzmann plot (BP) technique.

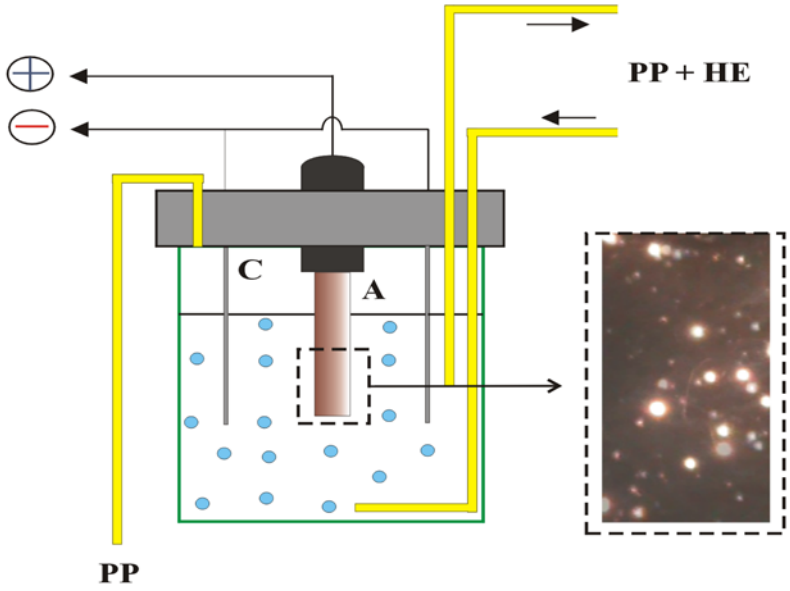

Figure 1. Schematic description of the PEO chamber and photo of micro-discharges recorded after third minute of PEO on Al-alloy anode. C – cathode, A – anode, PP – peristaltic pump, HE – heat exchanger.

2. Experimental

Magnesium-aluminium alloys AZ31 (wt.%, Al 2.5-3.5, Zn 0.6-1.4 and Mg balance) or AA5754 (wt.%, Mg 2.6-3.4, Si 0.4, Fe 0.4, Mn 0.5, Cr 0.3, Zn 0.2, and Al balance) were used as anode material in two separate experiments. Further, these two alloys will be named as Mg-alloy and Al-alloy, respectively. Rectangulary shaped anodes (dimensions 30 mm × 5 mm × 0.25 mm) were placed in electrolytic chamber, see Figure 1, leaving an active surface area of 1.5 cm^2. Two platinum wires (5 cm long and 1 mm in diameter) were used as cathodes. The PEO was carried out at 100 mA/cm^2 current density in voltage range (350-450) V. During PEO, the electrolyte circulated through the chamber-reservoir system (peristaltic pump and heat exchanger) and its temperature (≈ 20 ºC) was measured in the close vicinity of the anode. The water solution of 4 g/l $Na_2SiO_3{\cdot}5H_2O$ + 4 g/l KOH (pH ≈ 12.8) was used as an electrolyte.

Spectroscopic measurements were performed with three different spectrometers, see Table 1. The spectrum in a broad wavelength range (380 nm to 850 nm) was obtained by adding subsequent 43 nm spectral intervals recorded with spectrometer No. 1. This spectrometer was equipped with thermoelectrically cooled ICCD (-40 º C). The H_β and the spectra of O II and Mg I lines used for BP were recorded with spectrometer No. 2, while Mg II and Al II lines were recorded with spectrometer No. 3, see Table 1. The spectrometers Nos. 2 and 3 were equipped with thermoelectrically cooled CCD (-10˚ C) detector. All spectral lines were recorded after third minute of PEO when the voltage

slowly increases with time [2]. The full-width-at-half-maximum (FWHM) of Gaussian-like instrumental profile of spectrometer No. 2 in the first diffraction order was 0.030 nm. The instrumental FWHM of spectrometer No. 3 in the first and in the second diffraction order was 0.028 nm and 0.014 nm, respectively. The image of anode surface was projected with unity magnification to the entrance slit of spectrometer using an achromatic lens (focal length 75.8 mm). A standard coiled-coil tungsten halogen lamp was used for a wavelength sensitivity calibration of all spectrometer-detector systems.

Table 1. Characteristics of spectrometers and CCD detectors.

	Spectrometer 1	Spectrometer 2	Spectrometer 3
Focal length (m)	0.3	0.67	2
Grating (grooves/mm)	1200	1800	651
Linear dispersion in first diffraction order (nm/mm)	2.7	0.83	0.74
Detector	iCCD (-40˚C)	CCD (-10˚C)	CCD (-10˚C)

3. Plasma diagnostics

Before the procedure of plasma diagnostics is explained, the short description of PEO processes is given. Intensive gas generation is observed after first several seconds from the beginning of PEO while after about one minute micro-discharges become visible, see Fig. 2 in [6,9]. With the time, micro-discharges become brighter and larger, while their number is reduced, see Fig. 2 in [9] and [12].

Integral PEO spectra with Mg- and Al-alloy are presented in Figs. 2a and 2b, respectively. Apart from intensity, no other difference in the investigated current density range (50-100) mA/cm^2 is observed. Since there is no change in relative line intensities or line shapes for the same observation time of the PEO, the study of PEO with Mg- and Al-alloy anode was performed only for the electrode current density of 100 mA/cm^2.

3.1 Electron temperature

One of important parameters for PEO characterization and evaluation of N_e is free electrons plasma temperature T_e. It is assumed that under our experimental conditions, electron excitation temperature T_{exc} measured from relative line intensities using BP technique is equal to T_e. This implies that upper energy levels of lines used for the BP are populated in accordance with Boltzmann distribution of free electrons. The discussion on the fulfillment of partial local thermal equilibrium in PEO microdischarges and criterion for the BP application is given in [5]. However, it is justified to apply BP technique only if spectral lines used for T_e diagnostics are optically thin. For that purpose we compared intensity ratio of Mg I lines within a multiplet with corresponding line strengths ratio, see e.g. [10], and a good agreement was found. This is an indication that Mg I lines used for BP are optically thin, see e.g. [11-13]. The spectral lines of O II were so weak that self-absorption test was not necessary to perform.

The BPs of Mg I and O II lines recorded during PEO of Al-alloy anode are given in Figs. 3a and 3b, respectively. The list and data of used Mg I and O II lines are given in Ref [6]. From the slope of linear fit through data points in Fig. 3a, T_e = 3970 K ± 4 % from Mg I lines is determined. This temperature is very low in comparison with T_e measured from O II lines, T_e = 33070 K ± 12 %, see Fig. 3b. The estimated T_e uncertainties are the result of intensity measurements and transition probabilities. An absolute error is impossible to determine without knowledge of line intensity evolution and decay during time of single breakdown. This statement is relevant for all other reported data. For Mg-alloy anode, the Mg I lines BP has the same slope and thus same temperature, as in the case of Al-alloy anode. With the same Mg-alloy anode we were unable to measure T_e from O II lines since their intensity was very weak.

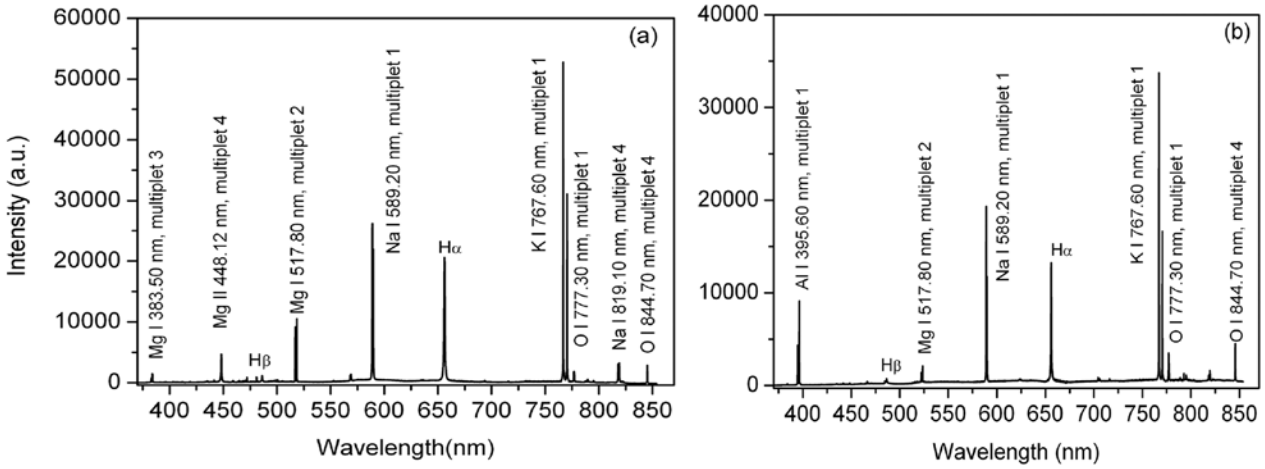

Figure 2. Typical PEO emission spectra in the spectral range 380 nm - 850 nm with: (a) Mg-alloy anode, (b) Al-alloy anode.

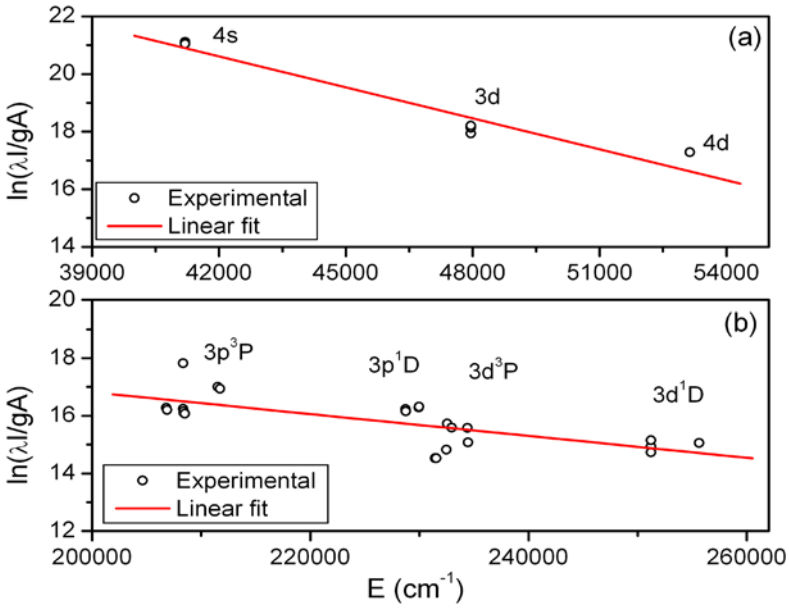

Figure 3. Boltzmann plot of: (a) seven Mg I lines and (b) twenty five O II lines, recorded during PEO with Al-alloy anode. The list of Mg I and O II lines with corresponding atomic data are given in [6].

Low T_e measured from Mg I lines is in a good agreement with recent results: T_e = 3300-7000 K reported in [14] and T_e = 3300 K measured from the BP of W I lines [10]. T_e determined from Mg I and O II lines is further used for N_e diagnostics from the width and/or shift of Al II 704.21 nm and Mg II 448.12 nm line and the H_β profile. High T_e from O II lines is in agreement with T_e results reported for PEO with pure Al anode [5]. The main difficulty in the interpretation of measured T_e data is how to determine the time of plasma evolution and/or decay when the Mg I lines used for BP are emitted. This difficulty will be better understood after reporting procedure and results of N_e measurement, see below.

3.2 Electron number density

It is important that the spectral line selected for N_e measurement is not self-absorbed, that it has good signal to noise ratio and does not interfere strongly with neighboring lines. For the selected line, reliable theoretical Stark broadening data must be available. As in previous PEO studies [5,7,8], first two hydrogen lines of Balmer series are selected as potential candidates for N_e plasma diagnostics. It was shown that the H_α and the H_β can't be fitted with single profile but with two Lorentz profiles. It is well known that self-absorbed line profile may also be, to the certain extent, approximated with Lorentz profile [13]. Therefore, the self-absorption test described in [7] is applied here as well. In addition to the H_α, the procedure also involves the two-profile fit of the H_β. The test revealed the H_α profiles distorted by self-absorption and, if used for diagnostics, 4-5 times larger N_e would be detected in plasma. This is the reason why the H_β line profile was used for plasma N_e diagnostics in this study.

The H_β profile recorded from Mg-alloy anode and fitted with two Stark profiles obtained using the procedure described in [15] is presented in Fig. 4. The theoretical data used for fitting the H_β profile are taken from [16] and two plasma N_e values, $(1.2 \pm 0.3) \times 10^{15}$ cm^{-3} and $(2.3 \pm 0.6) \times 10^{16}$ cm^{-3}, were determined. With the Al-alloy, strong AlO molecular band is interfering with the H_β profile, see Fig. 2b in [5]. This interference is the obstacle to use the H_β profile recorded during PEO of Al-alloy.

Non-hydrogenic ion line profiles were recorded and analyzed as well during the course of this study. The experimental procedure for N_e diagnostics from non-hydrogenic line profiles is described in detail elsewhere [12]. During PEO with Al-alloy, the shape of Al II line belonging to $4s^3S - 4p^3P^0$ multiplet 3, see the inset in Fig 5a, is used for diagnostic purposes. As for Mg I lines, see Section 3.1, the line self-absorption check is carried out using relative line intensities within multiplet. Within experimental uncertainty, strongest and medium intensity line show theoretical line intensity ratio 5:3, see line strength values in [10]. Thus, the strongest Al II line at 704.21 nm is selected for N_e diagnostics. The appearance of a small bulge on the blue wing of Al II lines, which makes lines asymmetric, was detected. Since the profiles of ion lines are not expected to be asymmetric, see e.g. [17], we carried out search for the cause of asymmetry. After the comparison of Al II 704.21 nm line profile with other spectral lines, the spectrometer was excluded as potential source of Al II lines asymmetry. The fitting of experimental profile with two Lorentz profiles having different width and shift was performed as the next step, see Fig. 5b. The two profiles fit describes much better Al II 704.21 nm line profile than single Lorentz profile, compare residue of Figs. 5a and 5b. The line shift of Al II 704.2 nm line is measured as well. This was done in respect to Ne I 705.92 nm line. As predicted by the theory [17], the Al II line shift is towards shorter wavelengths.

The best candidate for N_e diagnostics during PEO of Mg-alloy was $3d^2D - 4f^2F^0$ multiplet 4 with an average wavelength 448.12 nm, see profile recording in Fig. 6. The presented line shape consists of two close line profiles at 448.11 nm and 448.13 nm. This wavelength difference however does not cause difficulty in an analysis of the overall profile since Stark broadened lines within multiplet have same profile shape, width and shift [17-19]. The influence of small wavelength difference of 0.02 nm to the line width measurement is within the precision of this experiment. As for Al II 704.21 nm line, Mg II 448.11 nm line profile was fitted first with one Lorentz profile, see Fig. 6a. The experimental profile shows blue asymmetry at the line pedestal with both wings exceeding best fit Lorentz profile, see also residue in Fig. 6a. There is no logical explanation for isolated ion line profile (energy level separation between upper energy level and nearest perturbing level is larger than the line width) to exhibit such behavior. Therefore, we performed the fitting of experimental profile with two mutually shifted profiles, see Fig. 6b. Two Lorentz profiles with different width and shift significantly improve the fitting procedure, compare residues in Fig. 6a and 6b.

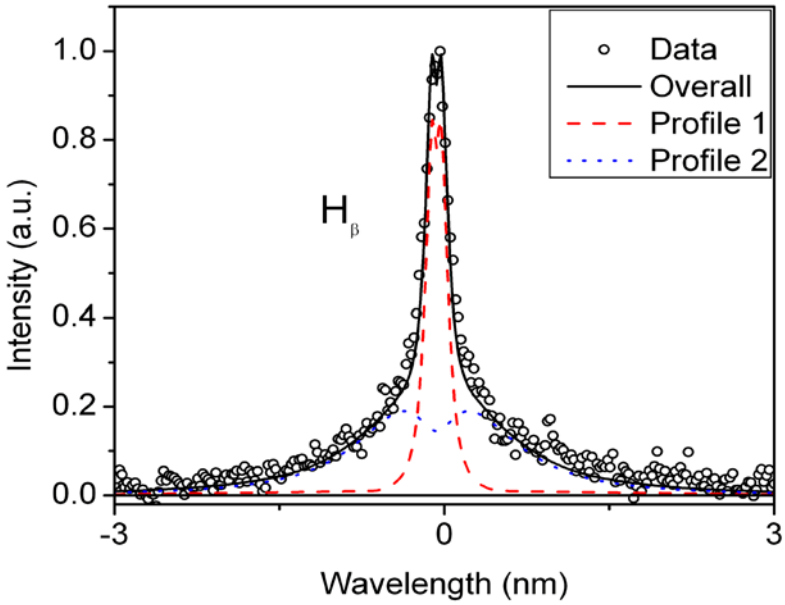

Figure 4. The H_β profile recorded during PEO with Mg-alloy anode and best fit with two Stark profiles. The instrumental profile halfwidth is 0.03 nm.

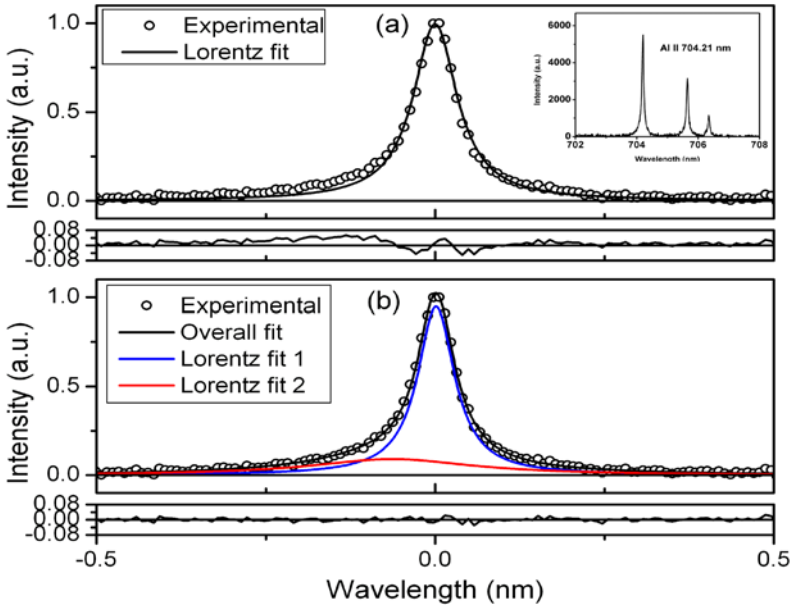

Figure 5. The experimental profile of Al II 704.21 nm line: (a) single best Lorentz fit and (b) two mutually shifted Lorentz fit. The line was recorded during PEO with Al-alloy anode. The instrumental profile halfwidth is 0.028 nm.

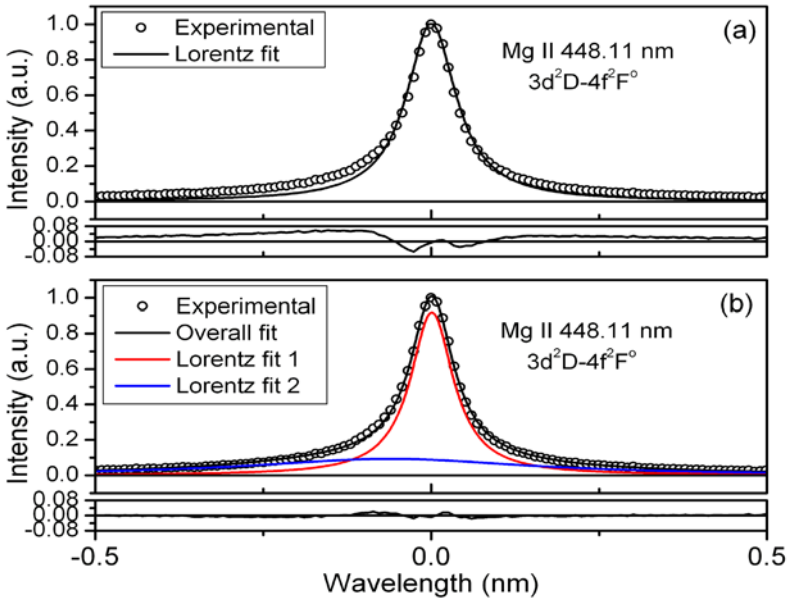

Figure 6. Mg II $3d^2D - 4f^2F^0$ line at 448.11 nm: (a) single best Lorentz fit and (b) two mutually shifted Lorentz fit. The line was recorded during PEO with Mg-alloy anode. The instrumental profile halfwidth is 0.028 nm.

4. Results and Discussion

The results of N_e measurement from halfwidths and shift of Mg II 448.11 nm and Al II 704.21 nm lines are shown in Table 2. Since N_e is determined from time and space averaged line profiles, it is difficult to estimate uncertainty of reported data. An estimated error in Table 2 is the result of experimental scatter, fitting procedure and uncertainty of theoretical data. An explanation of the procedure for N_e measurement from Mg II and Al II lines shall be given. First, the experimental line halfwidths are corrected for the contribution of Van der Waals broadening [20]:

$$w_{VW}[nm] = 5.925\times10^{14}\times K_1\times K_P\times p[mbar]\times T_g[K]^{-0.7} \quad (1)$$

$$K_1 = \lambda^2\times\left\langle R^2\right\rangle^{2/5} \quad (2)$$

$$K_P = \alpha^{2/5}/\mu^{3/10} \quad (3)$$

where p is the pressure, T_g gas temperature, λ is the wavelength of spectral line, $\left\langle R^2\right\rangle$ is the difference between the squares of the expectation values (in units of a_0) of the coordinate vector of the radiating electron in the upper and lower state of the transition, α is the mean atomic polarizability of the neutral perturber and μ is the atom-perturber reduced mass in a.m.u. Then, N_e is estimated from the comparison of experimental halfwidth and shift with Stark halfwidth or shift evaluated using formulas [11]:

$$w_t(N_e,T_e) \cong 2w_e(T_e)\times10^{-17}\times N_e \quad (4)$$

$$d_t(N_e,T_e) \cong d_e(T_e)\times10^{-17}\times N_e \quad (5)$$

In the above equations, $w_e(T_e)$ and $d_e(T_e)$ are electron impact half halfwidth and shift, respectively, calculated for $N_e = 10^{17}$ cm^{-3} and $T_e = 4000$ K [17]. Van der Waals halfwidth and shift are calculated under assumption: $p = 1000$ mbar and $T_e = T_g$ (T_g gas temperature). The perturber was Al or Mg atom depending on alloy. It was mentioned earlier, in relation to T_e measurement from the BP of Mg I lines,

that time interval during the ejection of metal plasma when Mg I lines are emitted is unknown. This time period may differ from the period when Mg II and Al II lines appear. In our case one has no other choice, since only several Mg I lines are available for T_e measurements while appropriate set of Mg II lines was not detected. In relation to the complex shape of Mg II and Al II lines used for N_e diagnostics, see Figs. 5 and 6, one can expect following steps in metal plasma evolution and decay. After breakdown and anode material evaporation, hot and dense metal plasma is ejected through micro-channel formed in oxide layer. In this time period observed Mg II and Al II lines are broad and shifted due to high plasma N_e. After ejection from micro-channel, plasma expands and cools down. This causes decrease of N_e and consequently narrowing of line profile and decrease of line shift. This narrower profile forms upper part of the overall profiles in Figures 5 and 6.

Finally, the atomic lines appear and quench at the end of this process. In relation to metal plasma ejection, the comment on low T_e = 3300 K measured from BP of W I lines [5] is given. During PEO of pure aluminium samples, tungsten was present in electrolyte solution [5] and the excitation of W I lines is a result of hot aluminium metal plasma interaction with electrolyte. This explains relatively low temperature measured from W I lines.

Assuming Saha equilibrium, an attempt is made to calculate T_e from N_e values presented in Table 2 using Saha equation for plasma at atmospheric pressure (electrolytic chamber is at atmospheric pressure). From N_e values for Mg- and Al-alloy of 1.6×10^{17} cm^{-3} and 1.2×10^{17} cm^{-3}, T_e of 7400 K and 6700 K is evaluated, respectively. Since the pressure at the opening of micro-channel, where the plasma of highest N_e is most likely ejected may be larger than one atmosphere, lower T_e for the same N_e would be determined from Saha equation. For example, T_e for Mg-alloy would decrease from 7400 K for one to 6000 K for ten atmospheres. In spite of pressure uncertainty, T_e in metal plasma evaluated from Saha equation is comparable with temperature derived using BP technique what is expected for Saha equilibrium.

Table 2. The results for N_e in 10^{16} cm^{-3} obtained from measured halfwidths and shift of Mg II 448.11 nm and Al II 704.21 nm lines.

Line	Anode	
	Mg-alloy	Al-alloy
Mg II 448.11 nm		
Profile 1	2.2 ± 1.0	*
Profile 2	16.0 ± 7.2	*
Al II 704.21 nm		
Profile 1	*	2.8 ± 1.3
Profile 2	*	12.0 ± 5.4
Shift	*	9.0 ± 4.0

Finally, let us summarize the main features of PEO microdischarges. The surface of metal-oxide layer has irregular micro structure, see e.g. Fig. 7 in [7], with sharp points where large electric fields appear and induce breakdown in gas bubbles always present in an electrolyte during PEO. This is the first process with lowest N_e determined from the H_β profile, see Section 3.2. The second process with $N_e \approx 2.2 \times 10^{16}$ cm^{-3}, determined also from the H_β profile, is related to the breakdown through dielectric oxide layer from the surface towards anode. The third process, deduced from Mg II 448.11 nm and Al II 704.21 nm lines, appears after breakdown of dielectric and is followed by ejection of metal plasma of anode material. With Ti and Ta anode, only breakdown through dielectric layer occurs, while melting and ejection of anode material does not occur. In such case, plasma has lower viscosity and lower weight than metal plasma and consists of molecules, atoms and ions belonging to water vapor and ablated dielectric material [6,7].

To conclude, let us point out that the determination of time evolution and time of appearance of each process numbered here from 1 to 3 is a key task for further advances in understanding PEO

processes. This would require time resolved spectroscopic study of a single micro-discharge what is not an easy task.

Acknowledgements
The author gratefully acknowledges the discussions with N.Konjević and S. Stojadinović. This work is supported by the Ministry of Education and Science of the Republic of Serbia under Project No. 171014.

References

[1] Yerokhin A L, Nie X, Leyland A, Matthews A, Dowey S J 1999 *Surf. Coat. Technol.* **122** 73.
[2] Sundararajan G, Rama Krishna L 2003 *Surf. Coat. Technol.* **167** 269.
[3] Moon S, Jeong Y 2009 *Corros. Sci.* **51** 1506.
[4] Narayanan T S N S, Park I S, Lee M H 2014 *Progress in Materials Science* **60** 1.
[5] Jovović J, Stojadinović S, Šišović N M, Konjević N 2011 *Surf. Coat. Technol.* **206** 24
[6] Stojadinović S, Vasilić R, Petković M, Belča I, Kasalica B, Perić M, Zeković Lj 2012 *Electrochim. Acta* **59** 354
[7] Stojadinović S, Jovović J, Petković M, Vasilić R, Konjević N 2011 *Surf. Coat. Technol.* **205** 5406
[8] Stojadinović S, Vasilić R, Petković M, Zeković Lj. 2011 *Surf. Coat. Technol.* **206** 575
[9] Jovović J, Stojadinović S, Šišović N M, Konjević N 2012 *J. Quant. Spectrosc. Radiat. Transfer*, **113** 1928
[10] http://physics.nist.gov/PhysRefData/ASD/lines_form.html
[11] Konjević N, Wiese W L 1976 *J. Phys. Chem. Ref. Data* **5** 259
[12] Konjević N 1999 *Phys. Reports* **316** 339
[13] Konjević N, Roberts J R 1976 *J. Phys. Chem. Ref. Data* **5** 209
[14] Hussein R O, Zhang P, Nie X, Xia Y, Northwood D O 2011 *Surf. Coat. Technol.* **206** 1990
[15] Žikić R, Gigosos M A, Ivković M, Gonzales M A, Konjević N 2002 *Spectrochim. Acta Part B* **57** 987
[16] Stehle C, Hutcheon R 1999 *Astron. Astrophys. Suppl. Ser.* **140** 93
[17] Griem H R 1974 Spectral Line Broadening by Plasmas, New York: Academic Press
[18] Wiese W L, Konjević N 1982 *J. Quant. Spectrosc. Radiat. Transfer* **28** 185
[19] Wiese W L, Konjević N 1992 *J. Quant. Spectrosc. Radiat. Transfer* **47** 185
[20] Konjević N, Ivković M and Sakan N 2012 *Spectrochim. Acta B* **76** 16